Pis'ma v ZhETF, vol. 103, iss. 6, pp. 428 – 432 © 2016 March 25

Plasmonic interferometer for spectroscopy of microwave radiation

V. M. Muravev[1)], *A. A. Fortunatov, A. A. Dremin, I. V. Kukushkin*

Institute of Solid State Physics of the RAS, 142432 Chernogolovka, Russia

Submitted 11 February 2016

We report the observation of photovoltage oscillations in back-gated two-dimensional electron systems when tuning the density under incident microwaves and in the absence of a magnetic field. The oscillations are periodic in the inverse of the square root of the density. They originate from the interference of screened bulk plasmons with a linear dispersion. This phenomenon can be exploited to devise a spectrometer-on-a-chip for millimeter waves. The influence of a perpendicular magnetic field is investigated and reveals a transformation of screened bulk plasmons waves into screened edge magnetoplasmons.

DOI: 10.7868/S0370274X16060035

Collective plasma excitations in low-dimensional electron systems have attracted interest for decades [1–6]. They have been commonly detected using far-infrared transmission spectroscopy [1–5] as well as inelastic light scattering [6]. Most of these experiments were carried out in the far-infrared and terahertz regimes because of restrictions imposed by the sample quality. Progress in sample growth has led to an increase of the electron mobility by several orders of magnitude compared to the samples on which initial experiments were reported. This improved quality has made it possible to investigate plasmons at much lower frequencies in the microwave regime. Such studies have unveiled a plethora of plasma-wave effects, some of which were unanticipated [7–14]. Notable recent examples in the two-dimensional electron system (2DES) include evidence for retardation in the plasmon spectrum [7, 15, 9, 14], demonstration of simplest elements of plasmonic optics [8, 10–12], and discovery of weakly damped plasma waves in the gated 2DESs [13].

The interference experiment demonstrated that the coherence of edge magneto-plasmons can persist over millimeter distances [16, 17]. By tuning the applied magnetic field, the velocity of the plasmons excited by the incident microwave radiation of fixed frequency was altered systematically. The interference condition was periodically fulfilled, so that field sweeping brought out B-periodic oscillations in the photo-voltage. It was recognized that this effect lends itself for the detection and spectroscopy of millimeter and sub-millimeter radiation [18, 19]. A Fourier transform of the photo-voltage oscillations reveals the frequency or spectrum of the incident radiation. Even though broadband detectors in the millimeter and sub-millimeter frequency regime are abundant, compact devices that simultaneous provide spectroscopic information are missing. The properties of plasmons in 2D electron systems may allow to fill this gap provided the cumbersome application of a magnetic field can be avoided.

In the present work we address whether interference can also be observed in the absence of a magnetic field by tuning the plasma velocity through a variation of the electron density. The density tunability is accomplished with the help of an *in-situ* grown semiconducting gate located underneath a modulation doped 2DES in order to minimize screening of the incident radiation. Indeed, sweeping the electron concentration under microwave radiation also produces an oscillating photovoltage signal that can be attributed to the interference of plasma waves. The nature of the plasma waves is investigated by applying a magnetic field. At zero or small magnetic fields the screening by the added back-gate drastically modifies the dispersion of the plasmons. Instead of the conventional square root dependence, the frequency grows linearly with increasing momentum. At large fields the plasmons are well described by the theory for edge magnetoplasmons derived in Ref. [20].

The experiments were carried out on an 18 nm wide GaAs/AlGaAs single quantum well, which was located 135 nm underneath the crystal surface. An n^+ GaAs back-gate was grown *in-situ* at a distance d of 765 nm below the quantum well. A schematic of the device geometry is depicted in the inset to Fig. 1. The device consists of a central 100 μm wide rectangular shape, which is covered with a metallic gate and terminates at each end in an ohmic contact referred to as the source or drain. Arms with a length l of 400 μm and a width W of 50 μm protrude from this central rectangle. These arms

[1)]e-mail: muravev@issp.ac.ru

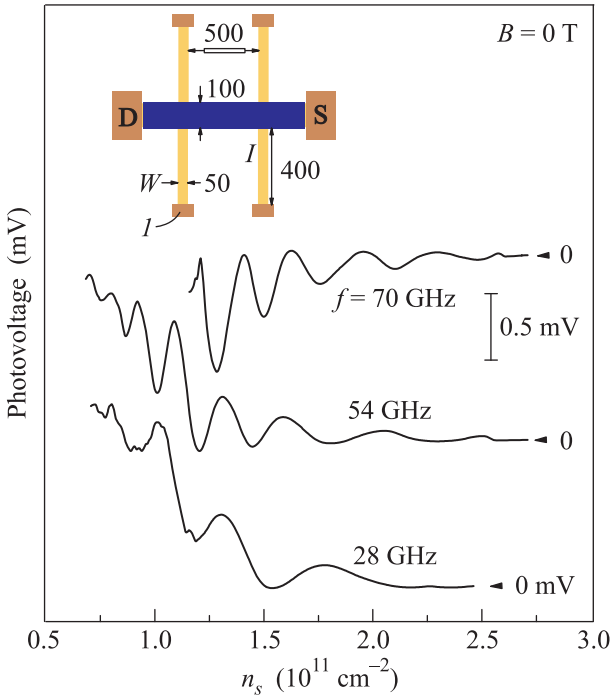

Fig. 1. (Color online) The photovoltage signal as a function of the electron density in the presence of 28, 54, and 70 GHz microwave radiation. Arrows indicate the signal level without radiation. Curves are offset vertically for clarity. The inset shows a schematic view of the sample geometry. All dimensions are in micron

too end in an ohmic contact, but are not covered by gate metal. They are 500 μm apart. The electron density n_s and electron mobility μ were tuned by applying a voltage to the back-gate. The density was varied from $0.5 \cdot 10^{11}$ to $2.8 \cdot 10^{11}$ cm^{-2}, while the mobility ranged between $1 \cdot 10^6$ cm^2/Vs and $5 \cdot 10^6$ cm^2/Vs for these densities. The sample was placed in the Faraday configuration near the end of a microwave waveguide with a rectangular cross-section of 19.0×9.5 mm^2 (WG17). The waveguide was submerged in the liquid helium of a cryostat containing a superconducting magnet coil. An Anritsu MG3690 generator provided microwave radiation with frequencies from 13 to 70 GHz with a typical output power from 10 to 0.1 mW. A sinusoidal voltage with an amplitude of 0.1 V was applied to the front gate in order to modulate the microwave induced photovoltage. Applied to the front gate voltage of 0.1 V corresponds to change in electron concentration of $0.6 \cdot 10^{11}$ cm^{-2}. The photovoltage was then detected at the modulation frequency with a lock-in amplifier. The experiments were carried out at a temperature of 4.2 K.

Fig. 1 depicts typical traces of the photovoltage as a function of the electron density for three different microwave frequencies. The experimental configuration is illustrated in the inset. The photovoltage is measured between the contact of one arm (marked as *1*) and a grounded drain contact (denoted with D) located at the end of the large rectangular mesa covered with gate metal. The traces have been offset vertically for clarity and the arrows indicate the zero signal level when no microwave radiation is incident on the sample. In each trace a series of oscillations is observed. We assert that the maxima originate from the constructive interference of plasma waves with wave numbers $q = m\pi/l$ between the ohmic contact of the arm and the gated region of the 2DES. Here, l is the distance between the gate and the contact of the arm, while m is an odd integer. According to the dipole approximation homogeneous incident radiation can only excite modes with odd values of m [15]. The ohmic contact and the partially depleted 2DES underneath the gate represent very different boundary conditions for the plasma waves. This difference has been held responsible for rectification of the high frequency signal and the appearance of a dc-photovoltage [16]. This interference picture is corroborated in the remainder of the manuscript by investigating in more detail the density and frequency dependence of the photovoltage oscillations and the nature of the plasma modes.

Plasma waves in the 2DES possess a dispersion which was calculated long ago [21, 22]:

$$\omega_p^2(q) = \frac{n_s e^2}{2m^* \varepsilon_0 \varepsilon(q)} q. \qquad (1)$$

Here, n_s and m^* are the density and the effective mass of the two-dimensional (2D) electrons, while ε_0 and $\varepsilon(q)$ are the permittivity of vacuum and the effective permittivity of the surrounding medium. It predicts a square root density dependence of the plasmon frequency. The dispersion on the other hand is strongly influenced by the effective permittivity and has been verified in experiments for different dielectric environments and sample geometries [2, 1, 23]. To understand the properties of the plasma waves involved in our investigation the experiment of Fig. 1 was repeated for a large set of microwave frequencies. The densities at which maxima occurred in the photovoltage are plotted in Fig. 2 (bottom panel) as a function of the incident microwave frequency. The data points fall onto eleven curves (dashed lines) which can be described well by the square root density dependence stipulated by Eq. (1). Each curve represents a mode with a different wave vector $q = m\pi/l$ ($m = 1, 3, 5, \ldots$) along the strip formed by the 2DES in between the contact and the gate. The wave vector dispersion is obtained by making a cut through graph 2A at a constant value of the density and plotted the crossing points of the verti-

cal line with the fitted square root curves. An example for $n_s = 1.5 \cdot 10^{11}\,\mathrm{cm}^{-2}$ is shown in the top panel to Fig. 2. The plasma dispersion turns out linear. The values of m were assigned such that in the limit of vanishing momentum also the plasmon frequency drops to zero in accordance with Eq. (1). Modes with $m = 7$ up to 27 were observed. A wave vector independent permittivity in Eq. (1) would yield a $\sqrt{q}$-dependence. The observed linear form indicates that the screening of the back gate layer plays an important role. The plasma waves in a 2DES with a nearby gate have been studied previously both in theory [22] and experiment [23–26]. According to the theory, a 2DES sandwiched between an AlGaAs layer of thicknesses d_1 at the top and an AlGaAs layer of thickness d followed by a conducting GaAs layer at the bottom, exhibits the following plasma spectrum in the limit of $qd \ll 1$ and $qd_1 \ll 1$:

$$\omega_{\mathrm{AP}}^2 = \frac{n_s e^2 d}{m^* \varepsilon \varepsilon_0} q^2. \qquad (2)$$

Here, $\varepsilon = 12.8$ is the permittivity of GaAs. Both validity constraints are fulfilled in our experiment. The dashed line in the top panel of Fig. 2 plots the dependence predicted by Eq. (2). The inaccurate description of the dielectric environment surrounding the 2DES as well as the non-ideal screening properties of the semiconductor based back-gate can easily account for the minor discrepancy with experiment.

We note that a linear dispersion was also reported for a plasma mode in a similar stripe geometry in the absence of a back-gate when the wave number of the excited mode obeyed the condition $qW \ll 1$, where W is the width of the strip (see inset Fig. 1) [27]. This mode was referred to as a 1D mode. In the opposite limit of $qW \gg 1$, the usual $\sqrt{q}$-dependence [9] was however recovered. We display the expected dispersion of the 1D mode for an ungated sample with the same dimensions as our sample and the chosen electron density of $1.5 \cdot 10^{11}/\mathrm{cm}^2$. The deviation is large and clearly the back-gate plays a crucial role for the appearance of a linear dispersion in the experiments here.

The photovoltage oscillations in Fig. 1 change with the frequency of the incident radiation. Hence, the device may serve as a "spectrometer-on-a-chip" provided the frequency dependence of the oscillations is understood. In Fig. 3 the values of $1/\sqrt{n_s}$ at which maxima in the photovoltage appear are plotted versus the mode index. The minima are also included and assigned even integers to account for the π-phase shift. Presenting the data in this manner shows that the extrema are spaced equidistantly. The periodicity $\Delta(1/\sqrt{n_s})$ is simply proportional to the inverse of the microwave frequency f (inset of Fig. 3). This follows also immediately from Eq. (2). A Fourier transform of the data straightforwardly yields the frequency of the incident radiation.

When introducing an external perpendicular magnetic field, Eq. (1) no longer describes the plasmon excitations in the 2DES and modifications to the photovoltage oscillations are bound to occur. Fig. 4 illustrates the oscillations observed in the presence of a magnetic

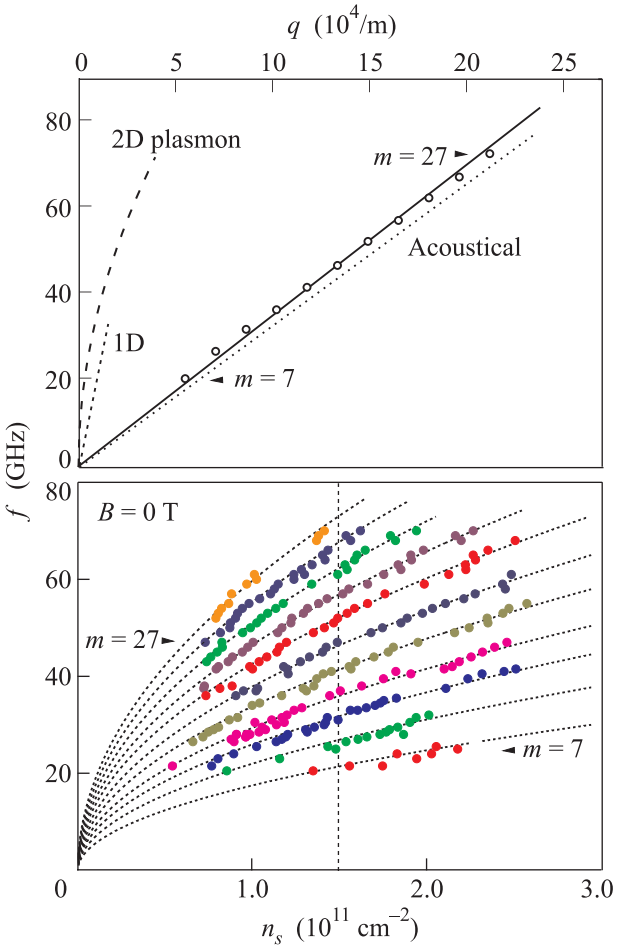

Fig. 2. (Color online) Bottom panel: the electron densities versus microwave frequency at which maxima occur in the photovoltage. The different colors refer to plasmon modes with a different wave number $q = m\pi/l$ along the length l of the strip in between the ohmic contact denoted as *1* in Fig. 1 and the top gate. Modes with $m = 7$ upto 27 were identified. Top panel: the dispersion of the plasmon at a fixed carrier density $n_s = 1.5 \cdot 10^{11}\,\mathrm{cm}^{-2}$ obtained from the crossings between the vertical dotted line and the eleven fit curves in bottom panel (open circles). The dotted line marks the theoretical prediction. For the sake of comparison the dispersion of 1D (long dash) and 2D (short dash) plasmons calculated for the same sample geometry but without back-gate are also included

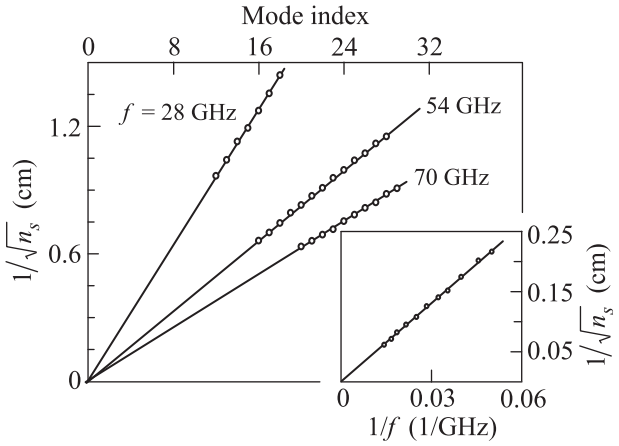

Fig. 3. The $1/\sqrt{n_s}$ values of the photovoltage maxima are plotted as a function of the mode index for three different microwave frequencies. Minima have also been included, but are assigned even integers to account for the π-phase shift. The inset shows the dependence of the $1/\sqrt{n_s}$-periodicity on the microwave frequency

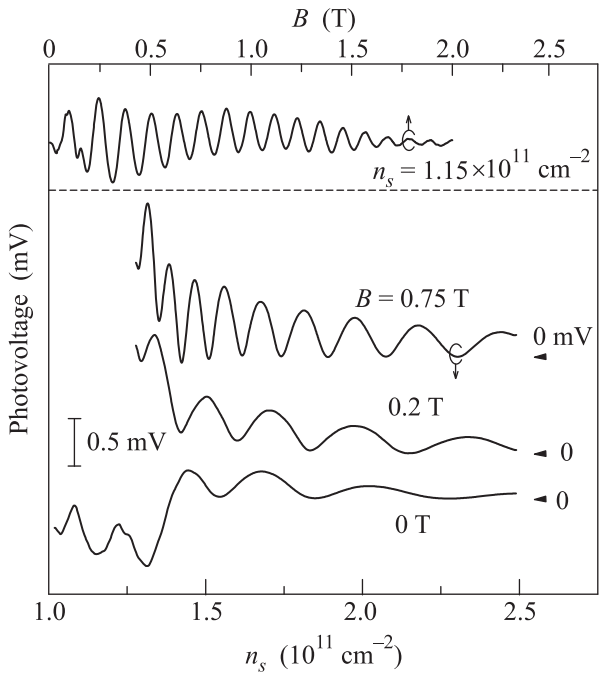

Fig. 4. Bottom curves: photovoltage oscillations when sweeping the carrier density in the presence of a fixed magnetic field and microwaves with a frequency of 53.1 GHz. The upper curve shows the signal when the magnetic field is swept, while carrier density and frequency are kept fixed. The photovoltage oscillates periodically with the B-field

field. For the data at the highest field, they are no longer equidistant when plotted on a $1/\sqrt{n_s}$-axis, but periodic in $1/n_s$ instead. These changes can be attributed to the modifications in the plasmon spectrum. The magnetic field evokes plasma waves, which are confined to the edge of the 2DES and propogate along the edge in the direction determined by the orientation of the field. The dispersion of these edge magnetoplasmons has been calculated by Volkov and Mikhailov [20] under the assumption of a uniform conductivity tensor across the sample and an abrupt drop in the conductivity at the sample edge:

$$\omega = \frac{\sigma_{xy}}{2\varepsilon_0\varepsilon^*} q\sqrt{\frac{d}{l^*}}. \qquad (3)$$

Here ε^* is the effective permittivity of the surrounding medium, which is approximately equal to the average permittivity of GaAs and vacuum; l^* is the width of the region along the 2DES boundary, which accomodates the density wave. It takes on values that are on the order of a few micrometers. The Hall conductivity is denoted as $\sigma_{xy} \propto n_s/B$. When interpreting the photovoltage oscillations as the manifestation of the interference of edge magnetoplasmons in between the ohmic contact and the region with top gate with wave numbers of the form $q = \pi m/l$ (m is again an odd number), we recover the proper $1/n_s$ density dependence. It is also instructive to sweep the magnetic field and record the photovoltage at fixed carrier density and frequency of the incident microwave radiation. An example is shown at the top of Fig. 4. The photovoltage oscillates periodically with magnetic field. The periodicity scales linearly with increasing density and is proportional to the inverse of the microwave frequency (not shown). Identical dependencies were reported in Ref. [8] on a geometry without gates. These dependencies lend further support to our interpretation as they follow immediately from Eq. (3). For a microwave frequency of 53.1 GHz for instance, we find that a transition from the $1/\sqrt{n_s}$ dependence to a $1/n_s$ dependence occurs near 0.5 T. After this field, the plasma excitation is confined sufficiently close the edge and is well described by Eq. (3).

In summary, we have demonstrated that microwave radiation incident on a two-dimensional electron system produces photovoltage oscillatons when sweeping the carrier density. The oscillations are periodic in the inverse of $\sqrt{n_s}$ or n_s depending on whether a perpendicular magnetic field is absent or present. They are attributed to the interference of acoustic plasmon modes in the absence of a field and the interference of screened edge magnetoplasmons in the presence of a fixed magnetic field. A Fourier analysis of the periodicity reveals the frequency of the incident microwave radiation and hence the sample can act as a microwave spectrometer-on-a-chip. Contrary to previously proposed schemes where a magnetic field had to be swept [8, 18, 19], tuning the carrier density can be easily accomplished. Success-

ful operation has been verified for microwave frequencies up to 100 GHz and no principal difficulties have been identified to extend operation even into the terahertz frequency range.

The authors gratefully acknowledge financial support from the Russian Science Foundation (Grant # 14-12-00599).

1. C. C. Grimes and G. Adams, Phys. Rev. Lett. **36**, 145 (1976).
2. S. J. Allen, D. C. Tsui, and R. A. Logan, Phys. Rev. Lett. **38**, 980 (1977).
3. D. Heitmann, Surf. Sci. **170**, 332 (1986).
4. S. J. Allen, H. L. Stormer, and J. C. M. Hwang, Phys. Rev. B **28**, 4875 (1983).
5. T. Demel, D. Heitmann, P. Granbow, and K. Ploog, Phys. Rev. Lett. **66**, 2657 (1991).
6. D. Richards, B. Jusserand, H. Peric, and B. Etienne, Phys. Rev. B **47**, 16028 (1976).
7. I. V. Kukushkin, J. H. Smet, S. A. Mikhailov, D. V. Kulakovskii, K. von Klitzing, and W. Wegscheider, Phys. Rev. Lett. **90**, 156801 (2003).
8. I. V. Kukushkin, M. Yu. Akimov, J. H. Smet, S. A. Mikhailov, K. von Klitzing, I. L. Aleiner, and V. I. Falko, Phys. Rev. Lett. **92**, 23 (2004).
9. I. V. Kukushkin, V. M. Muravev, J. H. Smet, M. Hauser, W. Dietsche, K. von Klitzing, and W. Wegscheider, Phys. Rev. B **73**, 113310 (2006).
10. H. Yoon, K. Y. M. Yeung, V. Umansky, and D. Ham, Nature **488**, 65 (2012).
11. W. F. Andress, H. Yoon, K. Y. M. Yeung, L. Qin, K. West, L. Pfeiffer, and D. Ham, Nano Lett. **12**, 2272 (2012).
12. G. C. Dyer, G. R. Aizin, S. J. Allen, A. D. Grine, D. Bethke, J. L. Reno, and E. A. Shaner, Nature Photon **7**, 925 (2013).
13. V. M. Muravev, P. A. Gusikhin, I. V. Andreev, and I. V. Kukushkin, Phys. Rev. Lett. **114**, 106805 (2015).
14. V. M. Muravev, I. V. Andreev, S. I. Gubarev, V. N. Belyanin, and I. V. Kukushkin, Phys. Rev. B **93**, 041110(R) (2016).
15. S. A. Mikhailov and N. A. Savostianova, Phys. Rev. B **71**, 035320 (2005).
16. V. M. Muravev, I. V. Kukushkin, J. H. Smet, and K. von Klitzing, JETP Lett. **90**, 197 (2009).
17. S. A. Mikhailov, Appl. Phys. Lett. **89**, 042109 (2006).
18. I. V. Kukushkin, S. A. Mikhailov, J. H. Smet, and K. von Klitzing, Appl. Phys. Lett. **86**, 044101 (2005).
19. P. S. Dorozhkin, S. V. Tovstonog, S. A. Mikhailov, I. V. Kukushkin, J. H. Smet, and K. von Klitzing, Appl. Phys. Lett. **87**, 092107 (2005).
20. V. A. Volkov and S. A. Mikhailov, ZhETF **94**, 217 (1988).
21. F. Stern, Phys. Rev. Lett. **18**, 546 (1967).
22. R. Z. Vitlina and A. V. Chaplik, ZhETF **81**, 1011 (1981) [Sov. Phys. JETP **54**, 536 (1981)].
23. V. M. Muravev, C. Jiang, I. V. Kukushkin, J. H. Smet, V. Umansky, and K. von Klitzing, Phys. Rev. B **75**, 193307 (2007).
24. P. J. Burke, I. B. Spielman, J. P. Eisenstein, L. N. Pfeiffer, and K. W. West, Appl. Phys. Lett. **76**, 745 (2000).
25. W. Knap, Y. Deng, S. Rumyantsev, and M. S. Shur, Appl. Phys. Lett. **81**, 4637 (2002).
26. M. Białek, M. Czapkiewicz, J. Wrobel, V. Umansky, and J. Łusakowski, Appl. Phys. Lett. **104**, 263514 (2014).
27. I. V. Kukushkin, J. H. Smet, V. A. Kovalskii, S. I. Gubarev, K. von Klitzing, and W. Wegscheider, Phys. Rev. B **72**, 161317 (2005).